Continuum polarization transfer in 500 MeV proton scattering and pionic collectivity in nuclei

L. B. Rees, J. M. Moss, T. A. Carey, K. W. Jones, J. B. McClelland, and N. Tanaka
Los Alamos National Laboratory, Los Alamos, New Mexico 87545

A. D. Bacher
Indiana University Cyclotron Facility, Bloomington, Indiana 47405

H. Esbensen
Argonne National Laboratory, Argonne, Illinois 60439

A complete set of polarization transfer observables was measured for inclusive 500 MeV proton scattering from ^{2}H, Ca(nat.), and Pb(nat.) at $\theta_{lab} = 18.5°$ ($q = 1.75$ fm^{-1}). The excitation energy ranged over the entire quasielastic peak from 20 to 100 MeV. Longitudinal and transverse spin-flip probabilities were extracted from the data. These have simple model-dependent connections to the spin-longitudinal and transverse response functions for the heavy targets. Detailed analysis of the data reveals no evidence for collective enhancement in the spin-longitudinal response function. The relation of this analysis to the interpretation of the European Muon Collaboration effect in terms of excess pions is discussed in detail.

I. INTRODUCTION

The response of nuclei to the spin-isospin fields $\sigma \times q e^{iq \cdot r}$ and $\sigma \cdot q e^{iq \cdot r}$ (where q is the momentum transfer) holds general interest for understanding the properties of hadronic matter. The transverse ($\sigma \times q$) and longitudinal ($\sigma \cdot q$) response functions have simple connections to the exchanges of ρ and π mesons between nucleons and between nucleons and Δ isobars, and are hence very relevant to current investigations into the effects of the isobar on nuclear properties.[1] Beyond this there are many issues connected with the spin-isospin resonances that carry over into the discussion of the role of quarks and gluons in the description of nuclear properties and interactions. One such issue, the interpretation of the European Muon Collaboration (EMC) effect,[2–6] is of direct relevance to the experiment reported here, and is discussed in detail herein.

The transverse continuum response function is now measurable over a wide range of q and ω (excitation energy) from the scattering of medium energy electrons.[7] Prior to this experiment the spin-longitudinal response function had been examined for only a few specific nuclear transitions between 0^+ and 0^- states—usually at the fixed, small momentum transfer and excitation energy available in nuclear beta decay.

The experiment reported here employs a new and general technique for the measurement of the spin-dependent response function.[8] It relies on measurement of a complete set of polarization transfer observables (PT) and is applicable, in principle, to nucleon inelastic scattering or charge-exchange reactions for the entire q-ω response surface including discrete states and the continuum. In this paper we present data derived from 500 MeV proton scattering for both the transverse and spin-longitudinal response functions for Ca and Pb at a momentum transfer

of 1.75 fm^{-1} for a range of ω from 20 to 100 MeV. Some of the data have been published in a previous letter.[9]

The range of q and ω dealt with here is particularly relevant to the nuclear pion field and the interesting possibility that it may confer a collective enhancement to the spin-longitudinal nuclear response. This hypothetical collectivity can arise from the pion-exchange interaction if it becomes attractive near $q = (2-3)m_\pi$. Forms of this collectivity in decreasing order-of-magnitude range from pion condensation,[10] possibly operable in neutron stars, through precursors of condensation (critical opalescence),[11] to the slight pion excess proposed to explain the EMC effect.

The principle of the experiment is simple. For targets of ^{2}H, Ca(nat.), and Pb(nat.) one measures spin-flip probabilities (SFP's) (defined in Sec. III) which bear a simple, although model-dependent, relation to the spin-isospin response functions.[8,9] One then looks for differences in these observables between ^{2}H and the heavy nuclei. As in the EMC experiment, ^{2}H is assumed to be a free neutron-plus-proton target, and hence free of any collectivity which possibly occurs in the heavy nuclei.

In Sec. II we review the EMC effect and its interpretation in terms of excess nuclear pions. Section III describes the techniques of our experiment. Section IV presents the reaction/structure model and comparison to the experimental data. Section V discusses three possible refinements to the reaction model. And finally in Sec. VI we return to the EMC effect and discuss the impact of the present experiment on its understanding.

II. THE EMC EFFECT AND EXCESS NUCLEAR PIONS

The original EMC data along with older Stanford Linear Accelerator Center (SLAC) data[12] are shown in

Fig. 1 in terms of the A-corrected ratio of the F_2 quark structure functions of iron and deuterium as a function of the scaling variable x. In the EMC experiment deuterium is assumed to represent a free neutron plus proton target. The data provide clear evidence that the quark distribution of bound nucleons is not identical to that of free nucleons. In a recent experiment at SLAC (Ref. 13) an extensive range of targets was examined with 8–20 GeV electron deep-inelastic scattering. These data confirm the anomalous A dependence seen by the EMC group, except for the very interesting region of positive ratio for $x < 0.3$. There is a considerable difference in the range of momentum transfer between the two experiments. Until further evidence is presented, one cannot say whether or not the different behaviors observed in the low-x region represent a real discrepancy.

The region in which the ratio of Fig. 1 is greater than unity is of particular relevance to the interpretation of the EMC experiment in terms of excess pions. As was shown by Llewellyn-Smith,[3] if one takes a model in which nuclei are composed of nucleons (dressed with their free-state meson fields) and pions, the EMC effect at $x = 0$ is roughly the fractional pion excess. West[14] has shown that the above argument applies to any model which presumes nuclei to be composed of a number of identifiable constituents. Thus Fig. 1 implies about 15% excess pions in Fe.

To define the model more precisely, we use the equations of the pion excess model given by Stump, Bertsch, and Pumplin.[6] The difference between the iron and deuterium structure functions is

$$\delta F_2^{Fe}(x) - \delta F_2^{D}(x) = \int_x^1 dz \, \delta f_\pi(z) F_2^\pi(x/z)$$
$$+ \int_0^{1-x} dz \, \delta f_\pi(z) F_2^N[x/(1-z)]$$
$$- \delta n_\pi F_2^N(x) , \qquad (2.1)$$

where

$$\delta f_\pi(z) = f_\pi^{Fe}(z) - f_\pi^{D}(z) \qquad (2.2)$$
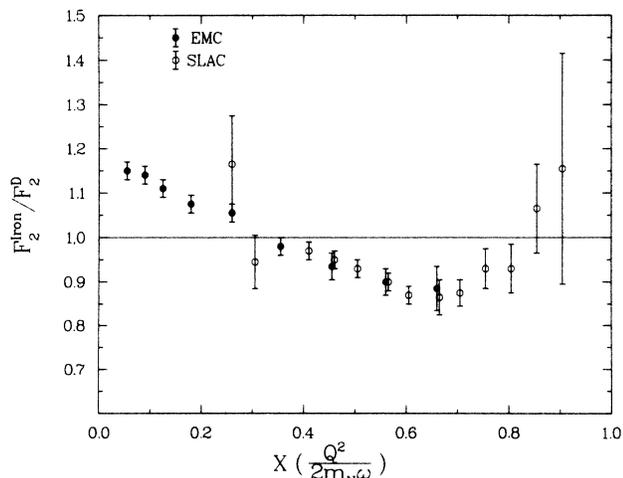
is the pion excess in Fe, and

FIG. 1. The A-corrected ratio of F_2 structure functions from the EMC collaboration (Ref. 3) and from SLAC (Ref. 12) as a function of the scaling variable x.

$$\delta n_\pi = \int_0^1 dz \, \delta f_\pi(z) \qquad (2.3)$$

is the integrated pion excess. In all calculations presented in Sec. VI we have made the simple assumption that $F_2^\pi(x) = F_2^N(x)$. The calculation of the pion excess distribution in a heavy target closely resembles that for a free nucleon given many years ago by Sullivan.[15] Specifically,

$$f_\pi(z) = \frac{3g_{\pi NN}^2}{16\pi^2} z \int_0^\infty dq_\perp^2 \int_0^\infty d\omega \frac{|\Gamma(t)|^2 t}{(t + m_\pi^2)^2} R_L(q,\omega) , \qquad (2.4)$$

with $q_z = z m_N + \omega$, $q = (q_\perp^2 + q_z^2)^{1/2}$, and $t = q^2 - \omega^2$, and where $g_{\pi NN}$ and $\Gamma(t)$ are the coupling constant and form factor at the πNN vertex, and $R_L(q,\omega)$ is the spin-longitudinal response function—the latter, of course, being the object of measurement of the present experiment. The normalization of the response function in this expression is chosen so that without residual interaction and ignoring Pauli blocking the total response is 1, i.e., $\int d\omega \, R(q,\omega) = 1$. When $R_L(q,\omega)$ is assumed to be enhanced due to collectivity in the pion-exchange interaction, δf_π is accordingly large. Typically, the maximum contribution to δf_π comes from the momentum transfer range of 300–400 MeV/c, the region in which pionic collectivity is expected to occur. This then is the range toward which the present experiment is directed.

It is important to point out that the EMC data come from muon scattering which probes the entire nuclear volume. The present proton scattering data are more localized to the nuclear surface. The response functions associated with the two types of experiments are therefore not identical. We will account for these differences in the interpretation of the present data as presented in Sec. IV.

III. EXPERIMENTAL TECHNIQUES AND ERRORS

In order to determine the longitudinal and transverse SFP's for ^2H, Ca, and Pb experimentally, it is necessary to measure complete sets of PT observables. These observables are defined through Eq. (3.1), which gives the polarization of the scattered particles, $\mathbf{P}$, in terms of the polarization of the incident beam, $\mathbf{P}_0$. This expression is of the most general form allowed by parity conservation.

$$\begin{bmatrix} P_S \\ P_N \\ P_L \end{bmatrix} = \left(\begin{bmatrix} D_{SS} & 0 & D_{LS} \\ 0 & D_{NN} & 0 \\ D_{SL} & 0 & D_{LL} \end{bmatrix} \begin{bmatrix} P_S^0 \\ P_N^0 \\ P_L^0 \end{bmatrix} + \begin{bmatrix} 0 \\ P(\theta) \\ 0 \end{bmatrix} \right) \frac{1}{1 + P_N^0 A_y} . \qquad (3.1)$$

Here the quantities L, N, and S refer to the longitudinal (beam direction), normal, and sideways ($\hat{N} \times \hat{L}$) directions in the laboratory. $P(\theta)$ is the polarization function and A_y is the analyzing power for the reaction. D_{NN}, D_{SS}, D_{SL}, D_{LS}, and D_{LL} are identical to the Wolfenstein parameters D, R, R', A, and A'.[16]

In order to measure the polarization transfer observables, all three components of the incident beam polariza-

tion must be available and all three components of the polarization of the scattered particles must be accurately determined.

The polarization of the incident beam was measured with two beam-line polarimeters. The magnitude was independently measured by a quench technique at the polarized ion source. Each polarimeter consisted of a thin CH_2 target with associated detectors to monitor proton-proton elastic scattering. The polarimeter remained in the beam during the course of the experiment so as to allow continuous monitoring of the beam polarization. The combination of these polarimeters and the quench technique allowed measurement of all three components of the beam's polarization simultaneously.

The polarization of the scattered particles was measured by the focal plane polarimeter (FPP) of the High Resolution Spectrometer (HRS) at Los Alamos Meson Physics Facility (LAMPF). The operation of the FPP is described in detail elsewhere.[17] Briefly, the system consists of a number of carbon blocks and sets of wire chambers upstream and downstream from these blocks. The carbon blocks serve as a double scattering target and the wire chambers permit the tracing of a particle's path before and after the double scattering. This arrangement allows for a full 2π angular acceptance for double scattering events. The analyzing power of the FPP is a function of the energy of the particles entering the FPP and hence varies with ω. In our analysis, the analyzing power was measured at $\omega=0$ and the energy dependence calculated by using the parametrization of Cremans, who has used the methods of Ransome et al. with an enlarged data base.[18] The average analyzing power over the 4.5–21.0 deg range of double-scattering angles accepted in this experiment was about 0.3.

In order to reduce many possible systematic errors in the measurement of the spins of both the incident and scattered particles, the beam polarization was regularly cycled through normal and reverse spins.

Although Eq. (3.1) represents the scattering process, it does not include the effects of the spectrometer system. The first order effect is that of spin precession in the dipole. More subtle effects such as finite acceptance and focusing were also taken into consideration.[17]

In addition, the contributions of small polarization components in directions other than the primary direction were at times significant and had to be considered in the extraction of observables. All uncertainties in beam polarization, scattered particle polarization, and analyzing powers of the beam line polarimeters, FPP, and target were included in the analysis of experimental errors. The most important sources of systematic error were uncertainties in the false asymmetries and analyzing powers of the beam line and focal plane polarimeters. In all cases these quantities were known to better than about 1%. Sufficient data were taken to reduce statistical uncertainties to approximately the same level as systematic uncertainties.

Our experiment measured polarization transfer observables across the quasielastic peaks of ^2H, Ca, and Pb. The incident energy was chosen to be 500 MeV since at higher energies the distorted-wave impulse approximation

(DWIA) effective interaction is increasingly dominated by spin independent terms and at lower energies the precession of the HRS effectively prevents measurement of L type components of the emergent particle's polarization. The scattered particles were detected at a laboratory angle of 18.5 deg, which corresponds to $q = 1.75$ fm^{-1}, the momentum transfer at which differences between longitudinal and transverse response is predicted to be greatest. In order to cover the most significant part of the quasielastic peak, five spectrometer settings were needed for the Pb target and three for the ^2H target. Only the region of the quasielastic peak for values of ω between 26 and 72 MeV was covered for the Ca target and hence only three spectrometer settings were used. We were able to accommodate relatively high count rates in our experiment since the modest energy resolution requirement of about 1 MeV allowed us to use fairly thick targets (1300 mg/cm^2 Pb and 250 mg/cm^2 Ca). In the case of ^2H, a cryogenic target was employed. The Ca target had been flashed with gold, but nevertheless had considerable oxygen and hydrogen contamination ($\sim20\%$ by weight). The effects of the hydrogen contamination were easily removed in the off-line analysis. Quasielastic scattering from oxygen could not be separated from the data of interest; however, since we are dealing with a nuclear surface localized scattering, this contamination was not considered to be serious.

The combinations of PT observables relevant to the present analysis are the longitudinal (L) and transverse (T) spin-flip probabilities defined below:
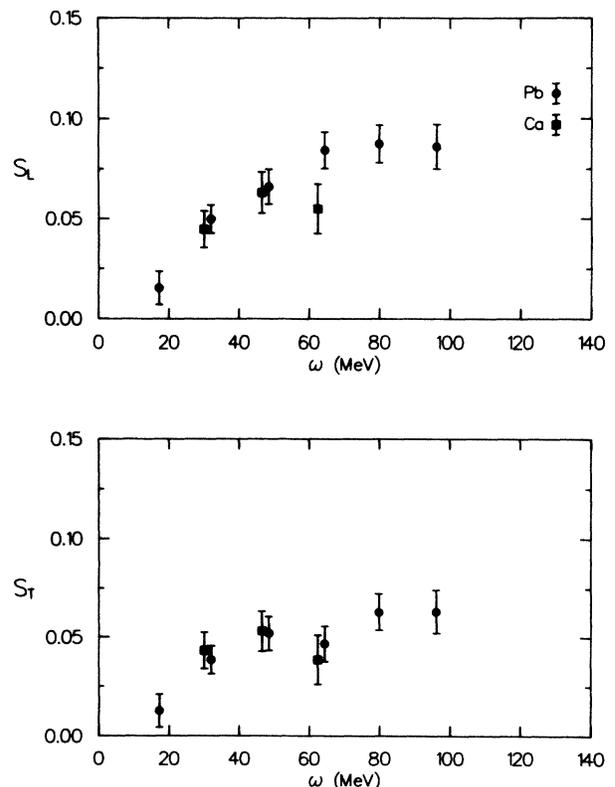

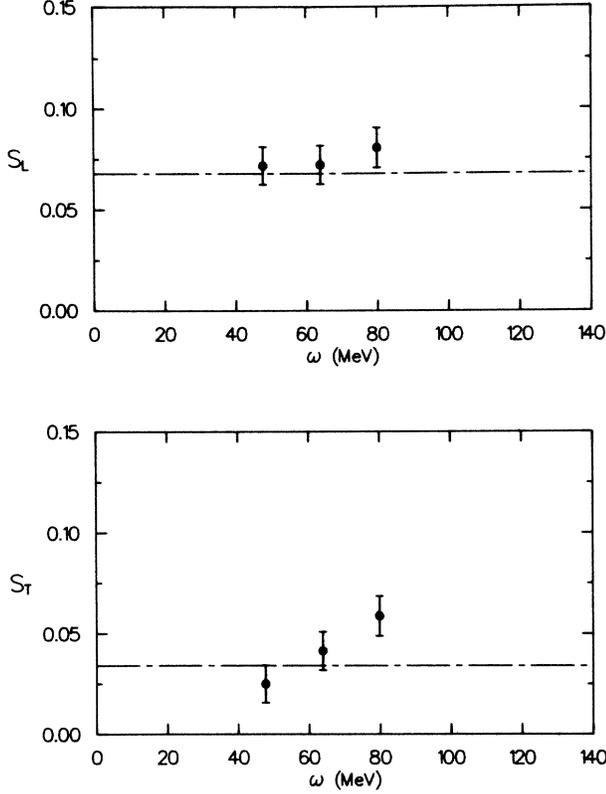FIG. 2. Longitudinal and transverse spin-flip probabilities in the (p,p') reaction at 500 MeV on Pb and Ca.

FIG. 3. Longitudinal and transverse spin flip probabilities in the (p,p') reaction at 500 MeV on ^{2}H. The lines are the average values of these quantities for p-n and p-p scattering from Ref. 19.

$$IS_L \equiv (I/4)[1-D_{NN}+(D_{SS}-D_{LL})\sec\theta_{\text{lab}}] , \qquad (3.2)$$

$$IS_T \equiv (I/4)[1-D_{NN}-(D_{SS}-D_{LL})\sec\theta_{\text{lab}}] , \qquad (3.3)$$

where I is the differential cross section. These quantities are shown for all targets in Figs. 2 and 3 as a function of ω; also shown are the phase shift solutions from Arndt's analysis.[19] (The individual values of D_{NN}, D_{SS}, and D_{LL} for lead and deuterium are shown in Ref. 9.)

IV. ANALYSIS AND DISCUSSION
A. General

It is clear from Figs. 2 and 3 that there are no significant differences between ^{2}H and the heavy targets for either S_L or S_T. The most important issue is, thus, how sensitively do the present data argue against collectivity in the isovector spin-longitudinal response function, and thus against excess pions as the source of the low-x EMC effect?

In this subsection we outline the model connection between the SFP's (experiment) and the spin-isospin response functions (theory) in the simplest single-scattering form. The following subsections present detailed comparisons of theory and experiment. In Sec. V we consider some refinements of the basic reaction model.

The model we employ is that developed by Bertsch and

Scholten[20] and extended by Esbensen and Bertsch.[21] The nuclear response functions are calculated in the semi-infinite slab model (SIS) using the random-phase approximation (RPA). Among the advantages of this method over the local-density Fermi-gas approach are that effects due to the physical nuclear surface can be accounted for explicitly. The SIS model contains nucleons in both bound and scattering states, so that response functions in the region near the Fermi surface are more accurately represented. Additionally, the reaction dynamics, based on the single scattering form of Glauber theory, can be implemented in a natural way. It is interesting to note that the results of the SIS are essentially the same as those of the calculation described in Ref. 9, which employed a Fermi gas approach using a local density distribution obtained from intranuclear cascade (INC) calculations. The specific connection of the reaction model to the data of the present experiment is as follows.

The free N-N scattering amplitude is taken to be

$$M(q)=A+B\sigma_{1n}\sigma_{2n}+C(\sigma_{1n}+\sigma_{2n})$$
$$+E\sigma_{1q}\sigma_{2q}+F\sigma_{1p}\sigma_{2p} , \qquad (4.1)$$

where the σ's are projections of the Pauli matrices along $\mathbf{n}=\mathbf{k}\times\mathbf{k}'$, $\mathbf{q}=\mathbf{k}'-\mathbf{k}$, and $\mathbf{p}=\mathbf{q}\times\mathbf{n}$; $\mathbf{k}$ $(\mathbf{k}')$ is the incident (outgoing) proton momentum direction. Then, with the definitions from Eqs. (3.2) and (3.3), for N-N scattering one has

$$I^{\text{N-N}}S_L^{\text{N-N}}=E^2 ,$$
$$I^{\text{N-N}}S_T^{\text{N-N}}=F^2 , \qquad (4.2)$$
$$I^{\text{N-N}}=A^2+B^2+2C^2+E^2+F^2 .$$

For N-nucleus scattering the ansatz of Bertsch, Scholten, and Esbensen yields

$$IS_L=I^{\text{N-N}}S_L^{\text{N-N}}R_L(q,\omega)N_e ,$$
$$IS_T=I^{\text{N-N}}S_T^{\text{N-N}}R_T(q,\omega)N_e , \qquad (4.3)$$
$$I=I^{\text{N-N}}R(q,\omega)N_e ,$$

with the axial-longitudinal, transverse, and total response functions defined as

$$R_L(q,\omega)=\sum_n |\langle n|f(\mathbf{r})\sigma\cdot\hat{q}e^{i\mathbf{q}\cdot\mathbf{r}}|0\rangle|^2\delta(\omega-E_n) ,$$

$$R_T(q,\omega)=\sum_n |\langle n|f(\mathbf{r})\sigma\times\hat{q}e^{i\mathbf{q}\cdot\mathbf{r}}|0\rangle|^2\delta(\omega-E_n) , \quad (4.4)$$

$$R(q,\omega)=\frac{C^2+B^2+F^2}{I^{\text{N-N}}}R_T+\frac{E^2}{I^{\text{N-N}}}R_L+\frac{A^2+C^2}{I^{\text{N-N}}}R_0 ,$$

where $\hat{q}$ is a unit vector,

$$R_0=\sum_n |\langle n|f(\mathbf{r})e^{i\mathbf{q}\cdot\mathbf{r}}|0\rangle|^2\delta(\omega-E_n) ,$$

and the summation indicates a sum over bound states and an integration over continuum states.

The effective number of nucleons, N_e, and the absorption function $f(\mathbf{r})$ contain the effects of attenuation of the proton waves in the nucleus; they are both evaluated consistently with Glauber theory.[20] For most of the discussion that follows, the precise value of N_e does not enter directly since we deal with ratios of response functions all

of which contain the same factor.

Rather than calculate the N-N quantities from phase shift solutions, we assume, as in the EMC experiment, that the ^{2}H data represent an average of the p-p and p-n observables. From Eq. (4.3) one finds, with $S^D = S^{N-N}$,

$$S_L^{Pb}/\langle S_L^D \rangle = R_L(q,\omega)/R(q,\omega) ,$$

$$S_T^{Pb}/\langle S_T^D \rangle = R_T(q,\omega)/R(q,\omega) ,$$

(4.5)

and

$$\frac{S_L^{Pb}/\langle S_L^D \rangle}{S_T^{Pb}/\langle S_T^D \rangle} = R_L(q,\omega)/R_T(q,\omega) .$$

(4.6)

The angular brackets on $S_{L,T}^D$ indicate that we have averaged the data over ω. This is consistent with our neglect of any nuclear structure contribution from deuterium. In Sec. V B we consider an alternative view.

In simple terms Eqs. (4.3) describe a reaction in which a beam of nucleons enters a nucleus, propagates in an eikonal fashion with attenuation, then scatters with momentum transfer q and energy loss ω (and exits the nucleus in a similar fashion). The transformation from center-of-mass to laboratory frame polarization observables is taken to be identical to that for free nucleons at the same angle, with the result that Eqs. (3.2) and (3.3) are valid for the quasi-elastic N-nucleus case.

In the model one also neglects current-current and spin-current couplings of the nucleons. This results in the appearance of only the static terms 1, $\sigma \cdot q e^{iq \cdot r}$, and $\sigma \times q e^{iq \cdot r}$ in the total nuclear response function. Considerable thought has been given recently to the origin of current couplings in the effective N-nucleus interaction in both the nonrelativistic[22,23] and Dirac formulations[24] of the impulse approximation. It is generally conceded that the current terms are small for medium-energy scattering and only by careful examination of particularly sensitive polarization observables will one be able to detect their presence. For 500 MeV inclusive quasifree scattering we expect the static approximation implied in Eqs. (4.3) and (4.4) to be adequate.

B. Analysis of R_L/R_T

It is appealing to analyze the ratio R_L/R_T for two major reasons. First, there is a great similarity in the usual theoretical treatment of these two spin-isospin responses, including the effects of short range correlations (see discussion below). Second, it is well established from continuum inelastic electron scattering that there are no *large* collective effects in the isovector transverse response function.[7] There may be a slight reduction in this channel, but even this small (10–20%) effect is not well established. For the present purposes we can be certain that values of R_L/R_T less than unity are not the result of a collective enhancement of the denominator.

If the experimental measurements corresponded to pure isovector transfer, it would be sufficient to calculate the right-hand side of Eq. (4.6) in the SIS model. However in (p,p') one must take the mixed $T=0$ and 1 nature of the process into account. This is accomplished using the isospin decomposition of the N-N interaction from the 500 MeV phase-shift solutions of Arndt.[19] The results for

$q = 1.75$ fm^{-1} are [in terms of the coefficients of Eq. (4.1)]

$$E_{T=1}^2/E_{T=0}^2 = 3.62 , \quad F_{T=1}^2/F_{T=0}^2 = 1.15 .$$

Thus the longitudinal interaction is dominantly isovector, but the transverse consists of nearly equal mixtures of isovector and isoscalar.

The quantities which enter the experimental ratio of Eq. (4.6) are then

$$\tilde{R}_L = \frac{1}{4.62}(3.62 R_L^{T=1} + R_L^{T=0})$$

(4.7)

and

$$\tilde{R}_T = \frac{1}{2.15}(1.15 R_T^{T=1} + R_T^{T=0})$$

(4.8)

In the discussions which follow, all response functions with a tilde will indicate the appropriate isospin averaged quantities. Thus $\tilde{R}$ denotes the total isospin averaged response function.

In all calculations we have assumed that the spin-dependent isoscalar response functions are given by the free (noninteracting nucleon) functions. This is consistent with the known weakness of the isoscalar spin-dependent forces,[25] but not well established at large q.

The N-N interaction in the spin-isospin channel is, of course, crucial in our analysis. It is only through the isovector longitudinal response that we establish a relation between this experiment and the EMC effect. We will thus be very explicit in the assumptions made in the present calculations of both the (p,p') reaction[26] and the EMC effect.[27]

The N-N particle-hole interactions in the isovector longitudinal and transverse channels are, respectively, taken to be of the standard π and ρ exchange forms. To the pure meson exchanges one adds the usual δ function interaction $g'(\sigma_1 \cdot \sigma_2)(\tau_1 \cdot \tau_2)$ to account for short range effects. The complete interactions are then

$$V_{ph}^L = \frac{f_\pi^2}{m_\pi^2} \Gamma_\pi^2 \left[g' - \frac{q^2}{q^2 + m_\pi^2 - \omega^2} \right] (\tau_1 \cdot \tau_2)(\sigma_1 \cdot \hat{q})(\sigma_2 \cdot \hat{q})$$

and

$$V_{ph}^T = \frac{f_\pi^2}{m_\pi^2} \left[g' \Gamma_\pi^2 - C_\rho \Gamma_\rho^2 \frac{q^2}{q^2 + m_\rho^2 - \omega^2} \right]$$

$$\times (\tau_1 \cdot \tau_2)(\sigma_1 \times \hat{q})(\sigma_2 \times \hat{q}) ,$$

with

$$C_\rho = f_\rho^2 m_\pi^2 m_\rho^2 \simeq 2.18 ,$$

$$\frac{f_\pi}{4\pi} = \frac{m_\pi g_{\pi NN}}{8\pi m_N} = 0.08 \quad [g_{\pi NN} \text{ from Eq. (2.4)}] ,$$

$$\Gamma_{\pi,\rho} = \left[\frac{\Lambda_{\pi,\rho}^2 - m_{\pi,\rho}^2}{\Lambda_{\pi,\rho}^2 + q^2 - \omega^2} \right] ,$$

$$\Lambda_\pi = 1.3 \text{ GeV} \quad \text{and} \quad \Lambda_\rho = 2 \text{ GeV} .$$

All RPA calculations include explicit coupling of nu-

cleons and Δ's with the usual assumption made that $g'(NN)=g'(N\Delta)=g'(\Delta\Delta)$. The value of g' is reasonably well established near $q=0$, but essentially undetermined experimentally near $q=1.75$ fm^{-1}. In particular, critical opalescence experiments only eliminate the very highly collective values of g' less than about 0.5. Thus we have performed calculations with a range of possible values, $g'=0.55$, 0.7, and 0.9. The minimum possible in this model is $g'=0.4$, which would make nuclear matter unstable with respect to pion condensation.[1,11] The signature of pion condensation here is that the longitudinal response $R_L(q,\omega)$ diverges at $\omega=0$ for a nonzero critical value of q. The collectivity in the longitudinal channel and hence both R_L/R_T of the present experiment and the low-x enhancement of the EMC effect vary considerably over this range. This is clear in Fig. 4, where the complete SIS calculations are compared to the superratio of Eq. (4.6) [with definitions (4.7) and (4.8)]. (The EMC effect is considered later.) All calculations presented are for Pb. There is little sensitivity to the nucleus since the half-density region is dominant in the SIS (and local Fermi gas) calculations.

It is obvious that the largest value of g' is favored. We should emphasize that the errors of Fig. 4 are only experimental. The significance of the disagreement between the data and the calculations also depends on the "theoretical" error bars in the reaction theory (the SIS model). In

Sec. V we consider some corrections and modifications of the model which relate to this point.

C. Separate analysis of R_L and R_T

The simple ratios of Eqs. (4.5) may also be analyzed separately. The numerators are again the isospin average response functions of Eqs. (4.7) and (4.8). The denominator, $\tilde{R}$, is dominated by the isoscalar spin-independent response function, but is constructed to contain all spin-isospin contributions. The isoscalar response contains well-known collective giant resonances at small q and ω, and it is important to include the appropriate physics in this channel in the present analysis. Fortunately, the SIS model with a RPA response function reproduces the gross features of medium-energy p-nucleus continuum data very well. Figure 5 shows this model's ability to account for 800 MeV p-nucleus continuum data[28] near the momentum transfer of the present experiment (where absolute cross sections were not measured).

Comparison of the calculated simple ratios $\tilde{R}_{L,T}/\tilde{R}$ to experiment is shown in Fig. 6 for the three values of g'. Figure 7 shows the calculated individual response functions which are used to form the ratios (for $g'=0.55$). The decrease seen in Fig. 6(a) at small ω for the $g'=0.9$ curves is due to a small collective enhancement in the isoscalar response which contributes to the denominator. For the smaller values of g' the collective nature of R_L causes the ratio to rise in substantial disagreement with experiment. The $\omega=19$ MeV point is substantially below the $g'=0.9$ calculation in Fig. 6(a). This may indicate that the calculated isoscalar response is not sufficiently collective. Another possibility considered in Sec. V B is that there is an additional ω dependence not contained in the SIS calculations.

Whether one uses $\tilde{R}_L/\tilde{R}_T$ or $\tilde{R}_L/\tilde{R}$, the analysis based on the SIS calculations does not favor *any* collectivity in the spin longitudinal channel.

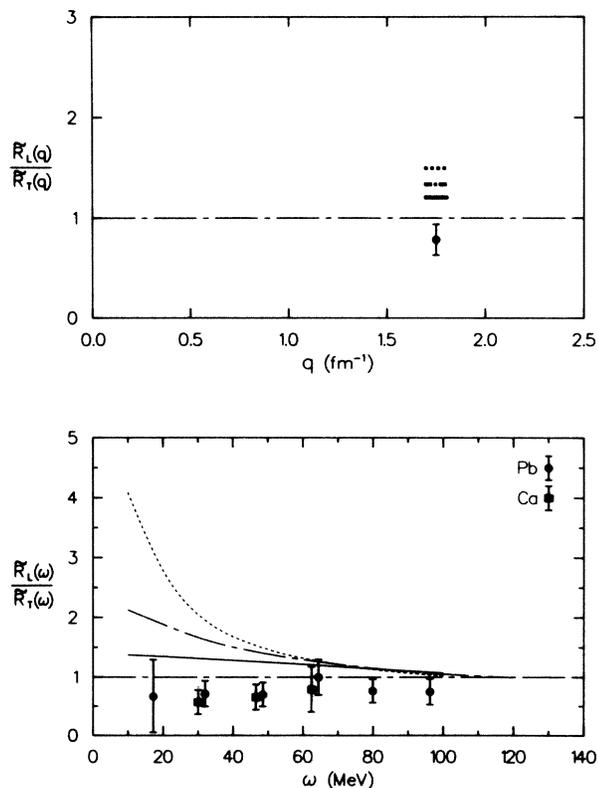The ratio $\tilde{R}_T/\tilde{R}$ is not reproduced particularly well by

FIG. 4. The ratio of spin longitudinal to transverse response functions as defined in the text. The top point and curves are obtained by averaging the lower values over ω. The calculations were performed using the SIS model with values of $g'=0.55$ (dotted), 0.7 (dotted-dashed), and 0.9 (solid).
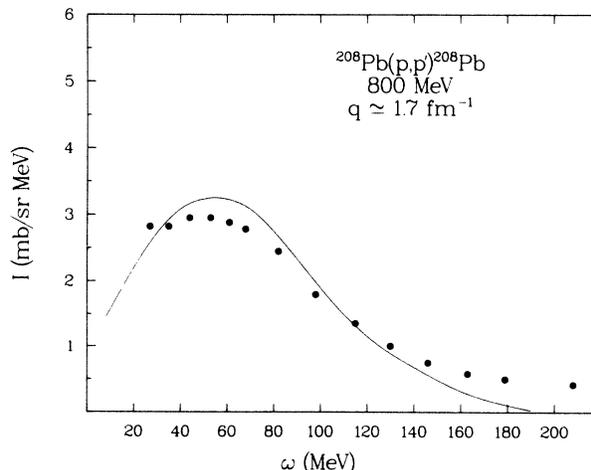

FIG. 5. Total continuum differential cross section from Ref. 28. The solid curve is a calculation using the SIS model.
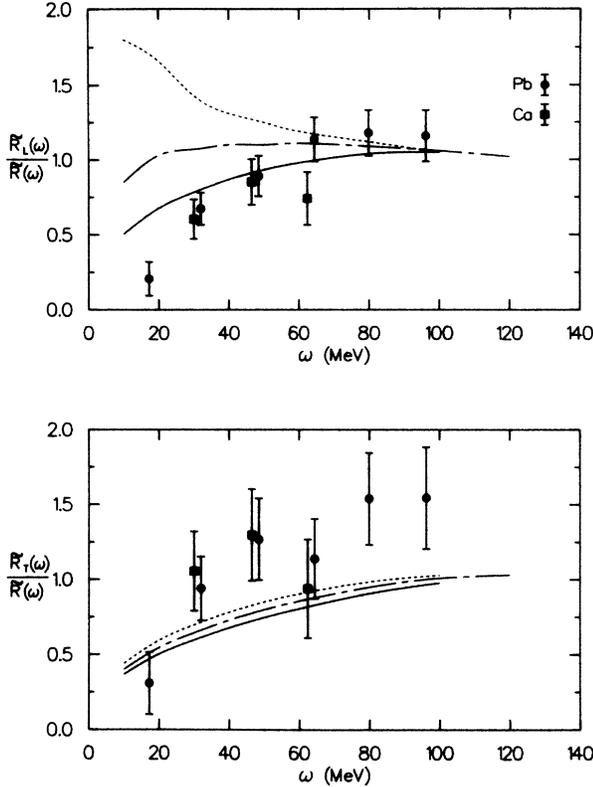
FIG. 6. Response function ratios described in the text. The curves are SIS calculations with $g'=0.55$ (dotted), 0.7 (dotted-dashed), and 0.9 (solid).

the calculations (there is little sensitivity to g'). Recall that the transverse response is a nearly equal mixture of isoscalar and isovector [Eq. (4.8)]. The discrepancy seen could be due to a small deviation of the isoscalar transverse response from its assumed free (noninteracting) value.
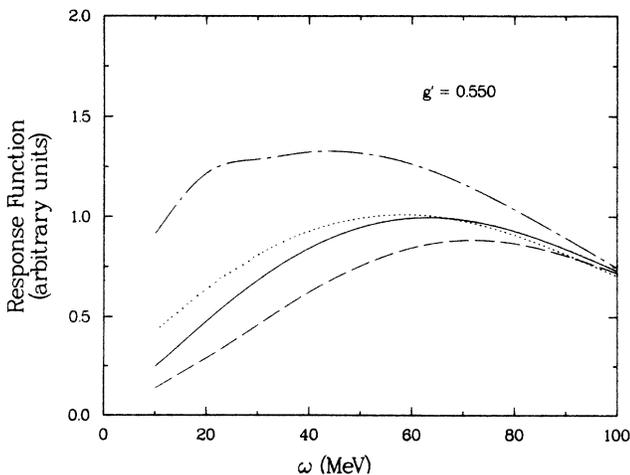

FIG. 7. Contributions to the SIS model calculations of the ratios of Eqs. (4.5) and (4.6) as defined by Eqs. (4.4). They are $\tilde{R}$ (dotted), $\tilde{R}_T$ (long dotted-dashed), R_L (short dotted-dashed), and R_{free} (solid). The calculations use $g'=0.55$.

V. EXTENSIONS OF THE SIS MODEL

This section considers three possible extensions of the analysis presented in Sec. IV. The calculations give some indication of the "error bars" on the theory discussed in Sec. IV.

A. Distortion effects

Equations (4.3) do not account for distortion effects other than eikonal attenuation of the initial and final nucleon waves. In particular, there is no account taken of spin-orbit (SO) distortion.

We note that there is considerable evidence against any large SO distortion effects in comparisons of the parameter D_{NN} (or S_{NN}) to distorted-wave Born approximation (DWBA) calculations. It is generally found that D_{NN} can be predicted by model analyses which neglect SO effects completely.[8,29-31] Perhaps the most convincing evidence comes from measurements of D_{NN} for collective isoscalar transitions.[8,29] Measurements to date give $D_{NN} \sim 1$, the value expected for a completely spin-independent scattering.

On the theoretical side, the most notable work to date is a recent model of continuum polarization observables by Horowitz and Iqbal.[32] They treat SO (and other) distortion effects in the eikonal approximation. Their conclusions, with the model's assumptions, are that S_L and S_T are not affected at all by SO distortion. This is not the case for other observables such as A_y and D_{LS}, where SO distortion effects are significant.

A remaining "distortion" effect not included in either the SIS or Horowitz-Iqbal models has to do with the differences in range of the transverse and longitudinal interactions. Simply stated, the long range of the one-pion exchange interaction may allow the proton to probe R_L further in the nuclear interior, thus affecting the ratio R_L/R_T. Evidence of such an effect has been suggested in analysis of small q data.[33] To be quantitative in assessing this possibility, we have performed DWBA calculations for ^{40}Ca in which the continuum scattering at $q=1.75$ fm^{-1} is represented by a high-spin harmonic-oscillator transition density. The oscillator parameter was chosen to yield a form factor peak at the half-density radius. Single particle transitions of the type $af_{1/2} + bf_{5/2} \to g_{9/2}$ ($0^+ \to 6^-$) were employed, with a and b chosen to yield either a purely longitudinal or purely transverse form factor at the peak of the cross section. Both DWBA and PWBA (PW denotes plane wave) calculations were then performed for both transition densities using the Love-Franey interaction.[34] The range effect is presumably absent in the PWBA calculations. The result is

$$(R_L/R_T)^{DW}/(R_L/R_T)^{PW}=1.05 .$$

Thus there is a slight favoring of the spin longitudinal response, indicating that the unit line of Fig. 4 might better be drawn at the above value (with a corresponding increase in the SIS calculations).

B. ω dependence in the ^{2}H data

In the SIS model the kinematics of the N-N system are treated in a manner which reflects the distribution of Fermi momenta in the target nucleus. For ω dependence of the differential cross section, this treatment is quite accurate as seen in Fig. 5. There is, however, no explicit ω dependence in the spin-dependent cross sections other than that assumed to arise from the response functions of Eq. (4.3). Our use of the deuterium data as the average p-p and p-n values implies $R_0 = R_L = R_T$ and hence no ω dependence. Figure 3 suggests that there is, in fact, an ω dependence in the deuterium data not contained in the model.

In order to investigate this as a possible kinematic effect due to the variation of q and ω over the quasielastic peak, we have constructed a knock-out model with the following properties. The cross section is given by

$$\frac{d^3\sigma}{d\Omega_1 d\Omega_2 dE_1} = K \left|\frac{d\sigma}{d\omega}\right|_{N\text{-}N} |\psi(-p_3)|^2 ,$$

where K is a kinematic factor, p_3 is the recoil momentum of the residual nucleon, ψ is the nuclear wave function of the struck particle, and $|d\sigma/d\omega|_{N\text{-}N}$ is the half-off-shell two-body differential cross section. For this quantity we
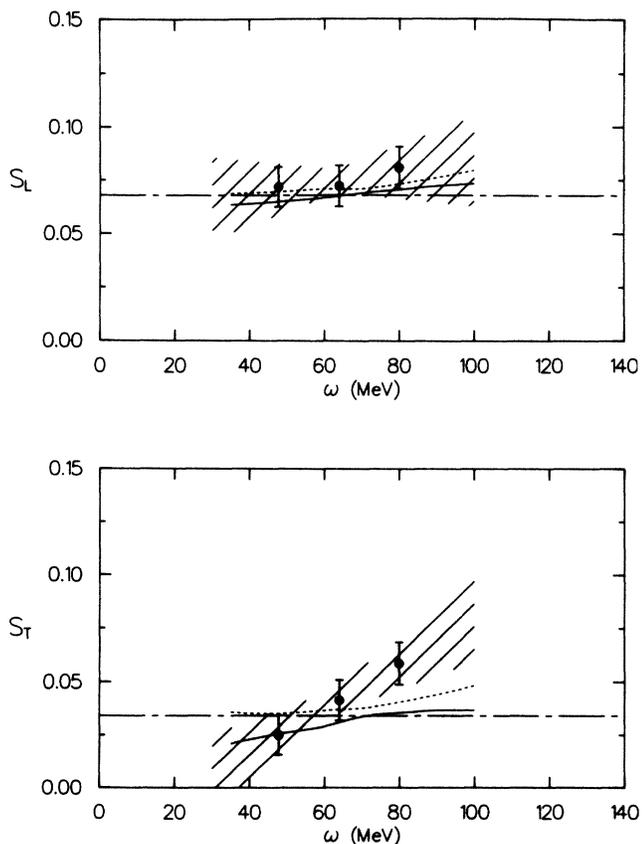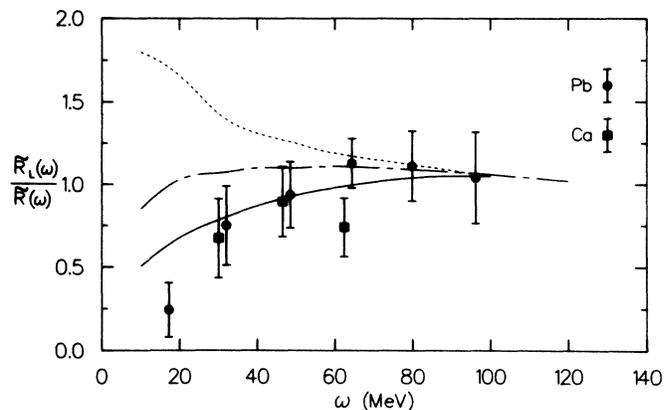

FIG. 9. The longitudinal response function ratio as described in Sec. V B.

used the on-shell cross section evaluated at energies given in either the final energy prescription (FEP, which uses the c.m. energy of the two emergent particle) or the initial energy prescription (IEP, which uses the energy of the incident particle and an on-shell struck particle boosted to the c.m. of the emergent particles). The polarization of the emergent particles and hence the polarization transfer observables are determined completely by the corresponding two-body values. In order to relate this calculation to experiment, one integrates the observables weighted by the cross section over the unobserved particle. The ω dependence of the observables arises from the ω dependence of the effective angles and energies at which the two-body cross sections are evaluated.

Figure 8 shows the comparison of the knock-out model to S_L and S_T for deuterium. The predicted linear increase with increasing ω is in good agreement with the data (the same trend is also seen in Ca and Pb). Because the slopes for S_L and S_T are nearly identical, this ω dependence has almost no effect on the superratio $\tilde{R}_L/\tilde{R}_T$. However, in analysis of $\tilde{R}_L/\tilde{R}$ one has a correction to the analysis of Fig. 6 which should be taken into account. We have accomplished this by performing a linear least-squares fit to the S_L data for deuterium and using the resulting $S_L^D(\omega)$ to replace $\langle S_L^D \rangle$ in Eq. (4.5). Statistical errors from the fit are included in the resulting error bars shown in Fig. 9. It is clear that the $g' = 0.9$ curve is still favored, but that increased size of the errors makes the case less dramatic, particularly if one ignores the $\omega = 19$ MeV point, where the SIS model may not have sufficient scalar-isoscalar collectivity.

FIG. 8. The calculated ω dependence of S_L and S_T for ^{2}H using the model described in the text. The dotted and solid curves use, respectively, the initial and final energy descriptions using the phase-shift solutions from Ref. 19. The cross-hatched region is derived from a linear least squares fit to the data.

C. Double scattering in the SIS model

It is straightforward to treat higher orders of scattering in the SIS model.[35] A look at the qualitative features of the nuclear response functions[21] reveals that the spin and isospin independent function R_0 has by far the largest cross section. This occurs in the small q,ω region, where the collective giant resonances dominate. Schematically then, one might consider the dominant double scattering process for either longitudinal or transverse spin flip at large q and ω to consist of a small q-ω collective scatter-
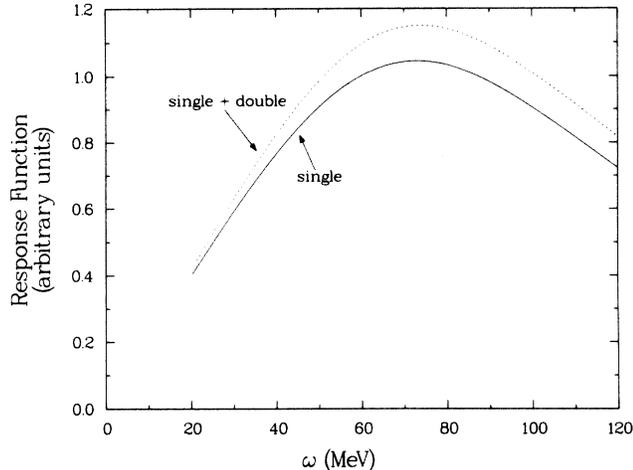
FIG. 10. Single and single plus double scattering contributions to the spin longitudinal response function.

FIG. 11. Calculations of the EMC effect using the model of Ref. 6. The curves are for $g'=0.55$ (solid), $g'=0.7$ (dashed), and $g'=0.9$ (dotted-dashed). They correspond to the same nuclear structure calculations presented in Figs. 4, 6, and 9.

ing followed or preceded by a large q-ω (near $q=1.75$ fm^{-1}, $\omega=60$ MeV) spin-flip event. In the limit that the spin-independent excitation occurs with no momentum transfer or energy loss, the kinematics of double scattering are identical to single scattering. The principal difference is that the probe is slightly more likely to sample the nuclear interior—*resulting in an increased sensitivity to the proposed pionic collectivity.*

We have not pursued this point quantitatively since the calculations presented here are still rather schematic. Figure 10 shows the single and single plus double scattering calculation of R_L in the SIS model. The observed $\sim 10\%$ increase shows that double scattering is not a large effect in the present experiment. Spin recoupling between scatterings and the increased sensitivity to the nuclear interior mentioned earlier were not taken into account in the calculations; hence the results cannot be applied quantitatively to the data. However, they do indicate that multiple scattering effects are unlikely to change the conclusions based on the single scattering form of the SIS model.

VI. CONCLUSIONS—EXCESS PIONS AND THE EMC EFFECT

We have described in detail the model relation of the polarization observables of the present experiment to the spin-longitudinal and transverse nuclear response functions. Analyses of the data both in terms of the ratios $\widetilde{R}_L(\omega)/\widetilde{R}_T(\omega)$ and $\widetilde{R}_L(\omega)/\widetilde{R}(\omega)$ show no evidence for collectivity in the nuclear pion field, such as would be reflected in an increase in $\widetilde{R}_L(\omega)$ at small ω. Using the $\pi+\rho+g'$ model for the spin-isospin response functions, our experiment favors $g'=0.9$ and strongly rules out values as small as $g'=0.55$.

The connection between the surface spin-isospin longitudinal response of the present experiment and the pion-excess model of the EMC effect has been outlined previously[3,4,6] and is summarized in Secs. II and IV. Calculations of the EMC effect[27] with the range of g' considered here are shown in Fig. 11. For these calculations we have
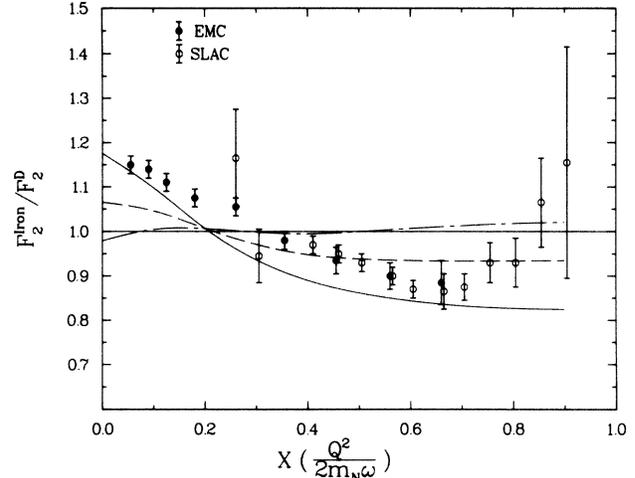
assumed $k_f=1.3$ fm^{-1} (full nuclear matter density) and that the pion and nucleon structure functions are identical. More realistic values for both[5,6] will reduce the $x=0$ intercept of the curves of Fig. 11. It is clear that the model analysis of this experiment favors values of $g'\gtrsim0.9$. This leaves little or no excess pions for the low-x EMC effect.

Although the present analysis of 500 MeV inclusive proton scattering is far from perfect, a number of points including spin-dependent distortion, kinematic effects in the deuterium data, and multiple scattering have been examined and have been found not to change the conclusion of the SIS model analysis.

Two further points relevant to this analysis have been discussed elsewhere.[36–38] First, the discrepancy between the "pionically collective" response functions and the present data is greatest at small ω where models based on the Fermi gas are suspect due to lack of binding energy effects.[36,37] The SIS model remedies this deficiency by including both bound and scattering wave functions for nucleons near the Fermi surface. Furthermore, the SIS model is quantitatively able to reproduce continuum data at values of ω even smaller than in the present experiment.[21] In short, the present analysis does not suffer any shortcomings in the small ω region at large momentum transfer.

The second point is that one needs to consider the possible mixing of transverse and longitudinal response functions in a finite nucleus (only in nuclear matter are they completely orthogonal). Such a calculation has been done in a harmonic oscillator basis for ^{40}Ca, and will be published shortly.[38] The result is that there is at most a 7% reduction in $\widetilde{R}_L/\widetilde{R}_T$ at $\omega=20$ MeV. The magnitude is thus far too small to have a significant impact on our conclusions.

Finally, we are aware that an alternative model[5] of the EMC effect in terms of excess pions exists which gives a

very good reproduction of the EMC and SLAC data. The nuclear matter theory from which the pions are generated bears little resemblance to that employed here. We believe that this model should be put to the test of reproducing the present experiment. Only by confronting low-energy data relevant to the meson/baryon description of nuclei will "conventional" nuclear physics models of high-energy physics results be truly tested.

[1]M. Ericson, Lecture Notes, International School of Physics, Erice, Italy, CERN Report No. TH-3625 (unpublished); E. Oset, H. Toki, and W. Weise, Phys. Rep. **83**, 283 (1982).
[2]J. J. Aubert *et al.*, Phys. Lett. **123B**, 275 (1983).
[3]C. H. Llewellyn-Smith, Phys. Lett. **128B**, 107 (1983).
[4]M. Ericson and A. W. Thomas, Phys. Lett. **128B**, 112 (1983).
[5]E. L. Berger, F. Coester, and R. B. Wiringa, Phys. Rev. D **29**, 398 (1984); E. L. Berger and F. Coester, Argonne National Laboratory Report No. ANL-HEP-PR-84-97, 1984 (unpublished).
[6]D. Stump, G. F. Bertsch, and J. Pumplin, in *Hadron Substructure in Nuclear Physics (Indiana University, 1983)*, AIP Conf. Proc. No. 110, edited by W. Y. P. Hwang and M. H. Macfarlane (AIP, New York, 1984), p. 339.
[7]Z. E. Meziani *et al.*, Phys. Rev. Lett. **54**, 1233 (1985).
[8]J. M. Moss, *International Conference on Spin Excitations in Nuclei*, edited by F. Petrovich *et al.* (Plenum, New York, 1984); J. M. Moss, Phys. Rev. C **26**, 2063 (1982).
[9]T. A. Carey *et al.*, Phys. Rev. Lett. **53**, 144 (1984).
[10]A. B. Migdal, Zh. Eksp. Teor. Fiz. **61**, 2209 (1971) [Sov. Phys.—JETP **34**, 1184 (1972)]; Rev. Mod. Phys. **50**, 107 (1978); R. F. Sawyer and D. J. Scalapino, Phys. Rev. D **7**, 953 (1972).
[11]J. Meyer-ter-Vehn, Phys. Rep. **74**, 281 (1981).
[12]A. Bodek *et al.*, Phys. Rev. Lett. **50**, 1431 (1983).
[13]R. G. Arnold *et al.*, Phys. Rev. Lett. **52**, 727 (1984).
[14]G. B. West, Los Alamos Report No. LA-UR-84-241, 1984 (unpublished).
[15]J. D. Sullivan, Phys. Rev. D **5**, 1732 (1972).
[16]L. Wolfenstein, Annu. Rev. Nucl. Sci. **6**, 43 (1956).
[17]J. B. McClelland *et al.*, Los Alamos Report No. LA-UR-84-1671, 1984 (unpublished).
[18]D. J. Cremans, M. A. thesis, University of Texas, 1983 (unpublished); R. D. Ransome *et al.*, Nucl. Instrum. Methods **201**, 315 (1982).
[19]R. A. Arndt and D. Roper, Virginia Polytechnic Institute Scattering Analysis Interactive Dial-In Program, solution SP84 (unpublished).
[20]G. F. Bertsch and O. Scholten, Phys. Rev. C **25**, 804 (1982).
[21]H. Esbensen and G. F. Bertsch, Ann. Phys. (Leipzig) **157**, 255 (1984).
[22]T. A. Carey *et al.*, Phys. Rev. Lett. **49**, 266 (1982).
[23]W. G. Love and Amir Klein, Proceedings of the LAMPF Workshop on Dirac Approaches to Nuclear Physics, Los Alamos Report No. LA-10438-C, p. 220, 1985 (unpublished).
[24]J. A. McNeil, Ref. 23, p. 160; J. R. Shepard, *ibid.*, p. 300; D. A. Sparrow *et al.*, Phys. Rev. Lett. **54**, 2207 (1985).
[25]H. Toki, G. F. Bertsch, and D. Cha, Phys. Rev. C **28**, 1398 (1983).
[26]H. Esbensen, H. Toki, and G. F. Bertsch, Phys. Rev. C **31**, 1816 (1985).
[27]Calculations were performed with a computer code provided by G. F. Bertsch.
[28]R. E. Chrien *et al.*, Phys. Rev. C **21**, 1014 (1980).
[29]S. Seestrom-Morris *et al.*, Phys. Rev. C **26**, 2131 (1982).
[30]J. B. McClelland *et al.*, Phys. Rev. Lett. **52**, 98 (1984).
[31]T. Taddeucci, in Proceedings of the 6th International Symposium on Polarization Phenomena in Nuclear Reactions, Osaka, Japan [J. Phys. Soc. Jpn. **55**, 156 (1986)].
[32]C. Horowitz and M. Iqbal, Phys. Rev. C **33**, 2059 (1986).
[33]W. G. Love, in Proceedings of the 6th International Symposium on Polarization Phenomena in Nuclear Reactions, Osaka, Japan, Ref. 31, p. 78.
[34]W. G. Love and M. A. Franey, Phys. Rev. C **24**, 1073 (1981).
[35]H. Esbensen and G. F. Bertsch, Phys. Rev. C **32**, 553 (1985).
[36]A. W. Thomas, in Proceedings of the LAMPF Workshop on Pion Double Charge Exchange, Los Alamos Report No. LA-10550-C, 1985 (unpublished).
[37]C. H. Llewellyn-Smith, Nucl. Phys. A **434**, 35c (1985).
[38]W. Alberico, A. Molivari, A. DePace, M. Ericson, and M. B. Johnson, Phys. Rev. C, in press.